



Study of elastic properties as function of temperature in an anisotropic cracked media

José J. da Silva Sobrinho* (Universidade Federal do Pará, Brasil), José J. S. de Figueiredo (Universidade Federal do Pará, Brasil & INCT-GP, Brasil), Lé K. Santos (Universidade Federal do Pará, Brasil).

Copyright 2018, SBGf - Sociedade Brasileira de Geofísica

This paper was prepared for presentation during the 8th Brazilian Symposium on Geophysics, held in Salinópolis, Brazil, 18 to 20 setembro 2018.

Contents of this paper were reviewed by the Technical Committee of the 8th Brazilian Symposium on Geophysics and do not necessarily represent any position of the SBGf, its officers or members. Electronic reproduction or storage of any part of this paper for commercial purposes without the written consent of The Brazilian Geophysical Society is prohibited.

Abstract

The study of the behavior of seismic wave velocities and their related anisotropy parameters is an important tool in the study of Earth's subsurface. The analysis of the influence of temperature in the elastic properties of synthetic rocks, for example, may be a good alternative to model the response of elastic properties of rocks surrounding deep wells and/or submitted to the process of steam injection. In this work, highly porous synthetic sandstones were produced, representing one isotropic and three cracked samples, and submitted to variable temperatures, being their elastic properties calculated during heating and cooling processes. P- and S-wave velocities decrease with increasing temperature, a behavior caused by changes in the background's stiffness and by the generation of secondary cracks inside the samples, whereas P- and S related anisotropy parameters were not affected by the changes in temperature, an indicative of random secondary cracks. Others indicatives of secondary cracking were the difference between seismic velocities during the heating and cooling processes.

Introduction

Seismic wave velocities are known to be a function of many factors, such as overburden and pore fluid pressure, lithology, porosity, composition and amount of pore fluids, pressure and temperature. Among these, lithology, porosity and pressure are considered to be the primary variables in affecting velocities (Timur, 1977). Nonetheless, the temperature effect plays a major role on seismic velocities under conditions of high temperatures, such as those found either in the steam injection process or in deep wells. Another factor of importance to seismic wave velocities is anisotropy. Vertical transversely isotropic (VTI) medium have been the subject of many studies along the years due to its great occurrence in sedimentary rocks and its importance to the oil industry. Thomsen (1986) has shown that, in the case of weak anisotropy (10%-20%),

the anisotropy of a medium can be described using three parameters: ϵ , γ and δ .

Investigating the temperature and pressure effects on seismic velocities of halite salt, Yan et al. (2016) concluded that the temperature effect on the velocities is dominant relative to the stress effect. Timur (1977) measured acoustic velocities in sandstone and carbonate samples as a function of temperature and found that the average decrease for a 100°C rise in temperature was 1.7% for compressional wave velocities and 0.9% for shear wave velocities. Kern (1978) investigated the effect of high temperature and high confining pressure on compressional wave velocities in rocks of different types and found that they generally decreases with temperature, but the rate varies according to the rock type. Furthermore, he concluded that, at higher isobaric pressures, the velocity drop as a function of temperature decreases and the velocity-temperature relations tend to become more and more linear functions.

Other studies have observed a decreasing of elastic modulus (Brotóns et al., 2013; Zhang et al., 2009) with the increasing temperature, which accounts for a decreasing in seismic velocities. Thermal gradient cracking has been found to be the dominant mechanism for fracture formation in experiments conducted at low confining pressure, resulting on the decreasing of seismic wave velocities with temperature (Jansen et al., 1993). Most of the previously mentioned works did not study the anisotropy dependence on temperature. Kern and Fakhimi (1975), however, studied the influence of temperature on anisotropy in various metamorphic rocks under high pressure conditions, and observed that fabric-induced seismic anisotropy is generally not affected by temperature. On this study, however, Kern and Fakhimi (1975) analyzed only P-wave anisotropy.

This study aims to further investigate the temperature influence on compressional and shear wave traveling in a VTI synthetic media, as well as the dependence of the Thomsen's parameters (ϵ , γ and δ) with respect to temperature. Measurements of traveltimes were performed through the ultrasonic method under atmospheric pressure as a function of temperature (ranging from 25 °C to 130 °C) in four cracked samples, constructed using the technique developed by Santos et al. (2017). Each synthetic sample has a different crack density which characterized different degrees of anisotropy, allowing us to analyze velocity changes with respect to temperature and crack density.

Methodology

The construction of the synthetic rock samples as well as the ultrasonic measurements were performed at the Laboratory of Petrophysics and Rock Physics - Dr. Om Prakash Verma (LPRP) at the Federal University of Pará, Brazil. The following methodology description corresponds to the production of fractured or cracked synthetic sandstones.

Sample preparation

We employed the methodology developed by Santos et al. (2017) for crafting synthetic VTI samples which is based on: cement, sand, styrofoam and paint thinner. Four samples were constructed with different crack densities.

Table 1 shows the number of cracks per layer and the crack density of each sample. In order to ensure that samples had the same composition, so that the differences in elastic properties were caused only by different crack densities, all samples were crafted simultaneously at the same mold, as it can be seen in Figure 1.

Table 1: Crack densities of the samples evaluated using Equation 1.

Sample	Cracks per layer	Crack Density
REF	-	-
L1	14	4.0%
L2	21	6.0%
L3	28	8.0%

The mortar used in the samples construction was composed of 70% sand and 30% cement. Moreover, the proportion of water was kept constant to ensure samples homogeneity composition. The cracks were disposed on layers constructed one at a time. At first, we filled the mold with a 2 cm layer of mortar and then placed penny shaped cuts of styrofoam that had a 0.5cm diameter and 0.1 cm thickness (Figure 1). We then filled another 0.5cm layer of mortar and placed another set of penny shaped cuts at the same area (4cm x 4cm) as before. This process was repeated until we had 7 layers with cracks spaced by 0.5cm. Finally, we filled the last 2 cm thick layer totalizing a height of 7 cm.

Right after filling the first layer, nichrome resistances pairs were placed in the regions of each sample (Figure 1). Those resistances are part of the temperature control system which is described in Sobrinho et al. (2017). The location where the resistances were placed at the mold was chosen taking into account the 45° cuts made afterwards on the edges of the samples to enable 45° measurements. As a matter of fact, the dimensions of the samples were chosen so that a cross section of the XZ-plane would be approximately a square, which in turn would enable propagation in the 45° direction.

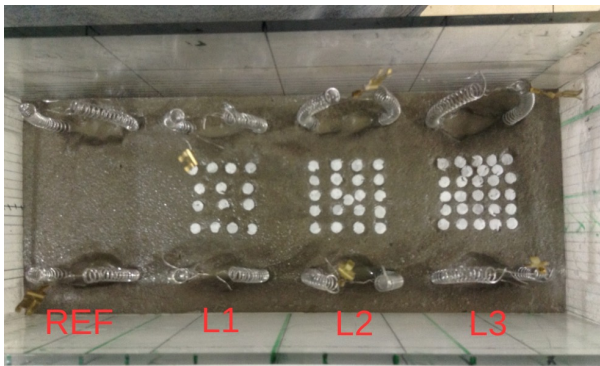


Figure 1: Crafting process of the samples showing the styrofoam discs disposed at the top of the mortar layer and the resistances positioned inside the mold.

The curing time of mortars produced with cement was about eight days (Garcia et al., 2011). Once the curing time was over we had the samples sawed apart. From Santos et al. (2017), to create penny-shaped voids, a chemical leaching using paint thinner was performed. The

samples were left immersed in paint thinner for around 24 hours and some samples were cut in order to verify the absence of styrofoam at the cracks. As the styrofoam is a polymer made by 98 % of air and 2 % of polystyrene (Poletto et al., 2014), after the leaching a practically zero amount of polystyrene mass remains inside the fracture. The sample crack density was estimated by the modified Hudson (1981)'s equation given by

$$\varepsilon = N_i \frac{\pi h_i r_i^2}{V_m}, \quad (1)$$

where N_i is the total number of penny-shaped inclusions, h_i is the aperture (thickness) of inclusion, r_i is the radius of the inclusion and V_m is the model volume (only) occupied by cracks.

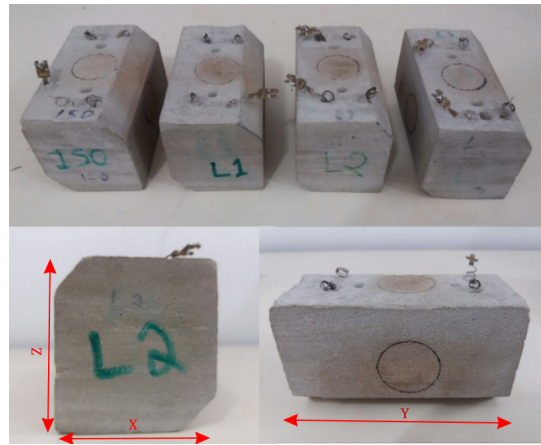


Figure 2: Picture of the four samples used in this study.

Ultrasonic setup and Data acquisition

The ultrasonic measurements were performed using the LPRP ultrasonic system with the same pulse transmission technique as realized in Santos et al. (2016) and Figueiredo et al. (2013). The sample rate by channel for all measures of P- and S-waveforms was $0.005\mu s$. Figure 3 shows the ultrasonic system. The system is compound by a pulser-receiver 5072PR and a preamplifier 5660B by Olympus, a 50 MHz USB oscilloscope by Handscope, and two transducers of 1 MHz (P-wave) and 500 kHz (S-wave) by Olympus.

The measurements were realized in the directions 0° , 45° and 90° , being 90° the direction parallel to the cracks, 0° the direction perpendicular to the cracks and 45° diagonal to the cracks. Figure 4 depicts the directions of propagation and polarization assigned on this study. All the measurements were performed with the sample temperature varying from $25^\circ C$ to $130^\circ C$. Temperature step was $15^\circ C$, which resulted in a total of 8 temperature values. In the direction 90° , two polarizations (z and y) were used in order to evaluate V_{s1} and V_{s2} . The measurements were carried out during the heating and the cooling for each sample, in an attempt to investigate the hysteresis of elastic wave velocities caused by temperature change.

At the beginning of the heating process the power was kept low (2-4%) to avoid the overshooting of the goal

temperature. The power was increased with the increasing sample temperature. At the maximum temperature, the power was about 10-11%. Afterwards, the power was gradually decreased in order to take ultrasonic measurements during the cooling process. Figure 5 depicts the experiment during the data acquisition.

To estimate P-wave velocities, we used the relation given as:

$$V_P(\theta) = \frac{L_P}{t_P(\theta) - \Delta t_{delay}}, \quad (2)$$

where L_P is the distance of P-wave propagation, $t_P(\theta)$ is the transmission time as a function of the angle with respect to the Z-axis of a P-wave, and Δt_{delay} is the delay time due to the S-wave transducers.

For S-wave velocities, the equation is similar to P-wave. They are given by

$$V_S(\phi) = \frac{L_S}{t_S(\phi) - \Delta t_{delay}}, \quad (3)$$

where L_S is the distance of S-wave propagation, $t_S(\phi)$ is the transmission travel time as a function of the angle polarization.

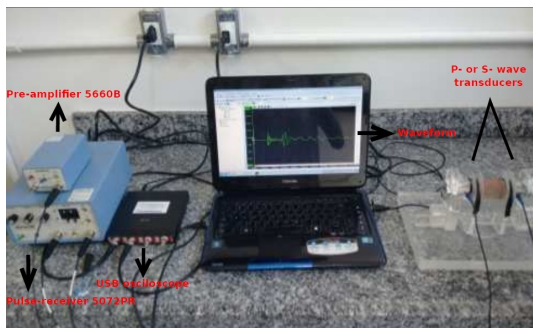


Figure 3: Ultrasonic measurement system showing the pre-amplifier, the oscilloscope, the pulse-receiver and the P- and S-wave transducers.

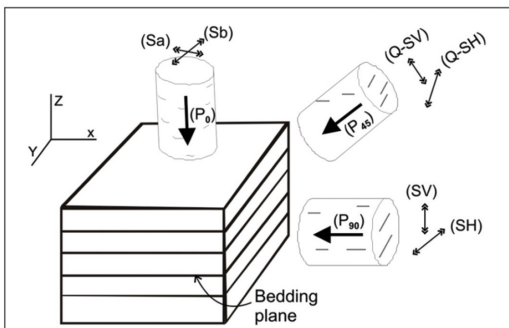


Figure 4: VTI media representation with directions of propagation and polarization assigned on this study. Source: [Martínez and Schmitt \(2011\)](#)

Results

Figure 6 shows velocities dependence with temperature during heating (red lines) and cooling (blue lines) processes for samples REF, L2 and L3. For all samples it

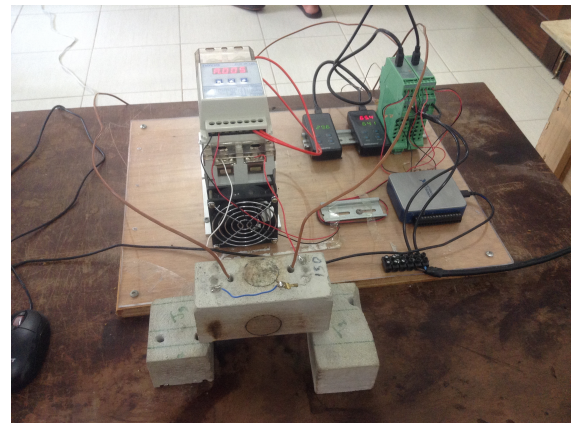


Figure 5: Temperature control system and sample during data acquisition.

was observed a decrease in velocities with the increasing temperature. Also, it is evident the existing of hysteresis in all the samples for all velocities, i.e., there is a variation of velocity for the same temperature when the sample is heating and cooling. Using the support of previous works to interpret these behaviors, such as the works of [Timur \(1977\)](#), [Kern \(1978\)](#) and [Jansen et al. \(1993\)](#), it can be said that they may be caused by the generation of microcracks inside the samples (secondary cracking), the coalescence of those microcracks and the decrease of the background stiffness of the samples. As expected, the opposite behavior occurs when the samples cooled. Since the microcracks generated by the heating process do not disappear when the samples are cooled down, it can be inferred that the behavior showed by the blue lines, where the velocities increased with the decreasing temperature, are solely or mostly related to the variation of background stiffness. Another indicatives of the secondary cracking and cracking coalescence is the fact that the velocities never return to their initial values after the cooling process.

Figure 7 shows the variation of P and S-wave velocities as function of both temperature and crack density represented by the sample labels. It can be seen that the gradient of velocity as a function of temperature and crack density points in the direction of minimum temperature and crack density, which is a expected behavior since velocity decreases with increasing temperature and increasing crack density.

Figure 8 shows the variation of the Thomsen's parameters (γ , ϵ and δ) as a function of temperature, for sample L2, during both the heating and cooling processes. The γ and ϵ values increase as the number of cracks of the samples increase, which is an expected behavior. In most of the cases, the γ and ϵ values show very close heating and cooling values, which is consistent with the observations made by [Kern and Fakhimi \(1975\)](#) that temperature does not noticeably reduce fabric-induced anisotropy. This may be caused by the fact that P-wave velocities in the 0° direction decrease at approximately the same rate as the 90° direction; the same occurs for S-wave velocities for different polarizations. This is an indicative that the secondary cracks generated during the heating process are randomly oriented. As for the δ parameter, it does not seem to show any correlation with temperature variation.

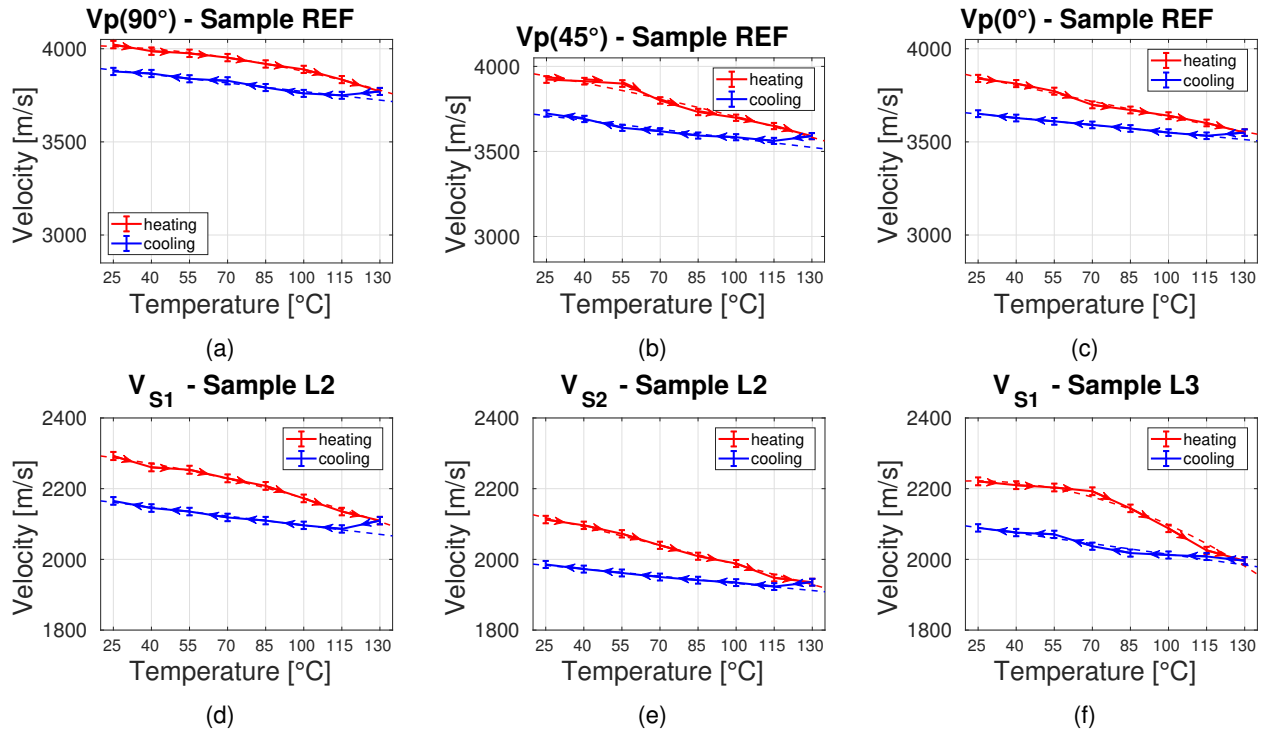


Figure 6: P-wave velocities in all directions for sample REF (a, b and c), S-wave velocities of sample L2 (d and e) and sample L3 (f) as function of temperature.

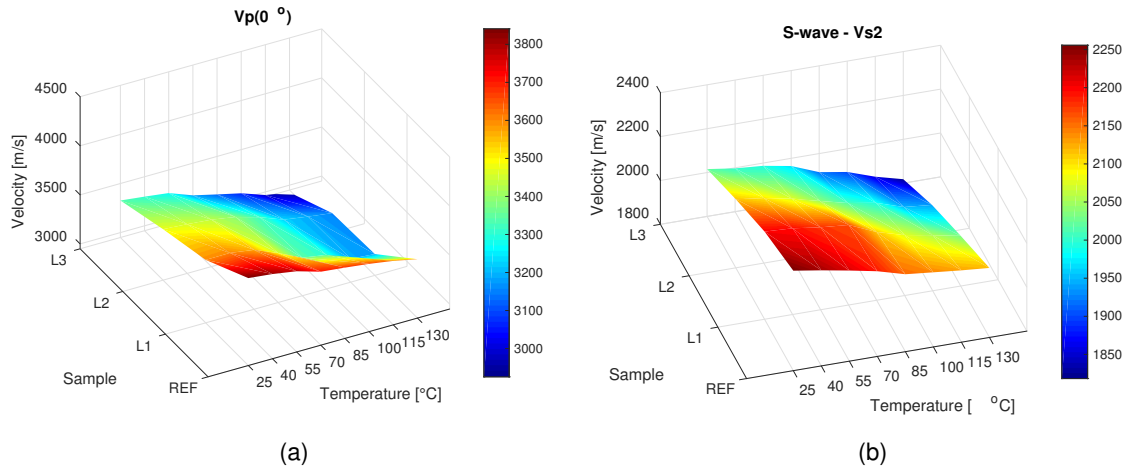


Figure 7: Elastic velocities (P and S) as function of temperature and crack densities shown by maps graphics. For all maps the highest velocity occurs when the temperature is 25° and the crack density is 0.

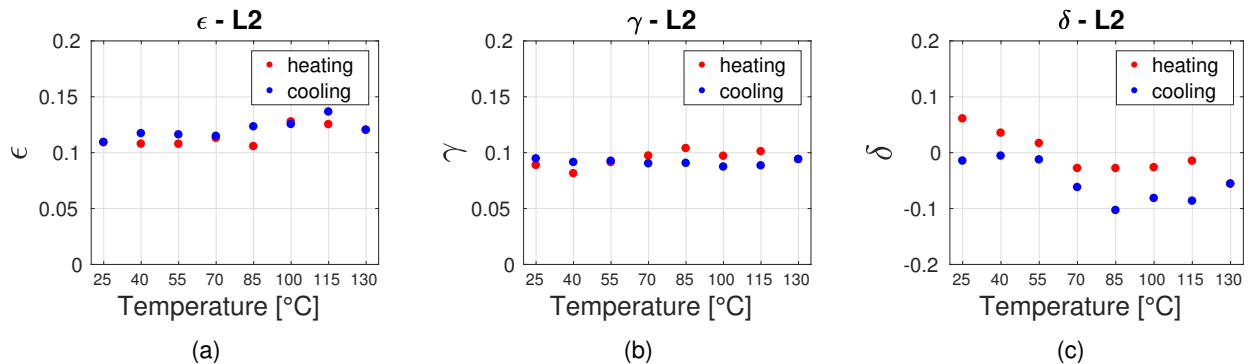


Figure 8: Thomsen's parameters as function of temperature for sample L2.

Conclusions

An ultrasonic procedure was performed on synthetic samples representing isotropic and cracked sandstones. They were constructed using cheap materials and a very simple construction methodology. The waveforms were acquired from the samples for different temperatures, which was possible by using a temperature controlling system. From the analyzes of the results, the following conclusions were obtained:

- The increasing temperature decreases the background stiffness and generates secondary cracks inside the samples.
- P-wave velocities had on average a 11% decrease for a 105°C rise in temperature, and P-wave velocity decreased approximately at the same rate on all directions of propagation.
- S-wave velocities had on average a 9% decrease for a 105°C rise in temperature, decaying at the same rate for both polarizations.
- Anisotropy parameters γ and ε presented very close values both for heating and cooling. They do not show a satisfactory pattern with the increasing and decreasing temperature, making their use as tools to model elastic properties as a function of temperature not applicable.

In addition to the conclusions obtained, it is worth highlighting the importance of this work as the first approach using porous synthetic rocks in the analysis of the influence of temperature in the behavior of elastic properties. The same approach may be repeated using rocks with different mineralogical composition and/or anisotropy symmetries.

Acknowledgments

The author would like to thank SBGf for the scholarship, and Ministério da Educação (PET- GEOFÍSICA-UFFPA), CNPq (Grant number 459063/2014-6) and PROPESP-UFFPA for financial support. We also would like to thank the Faculdade de Geofísica as well as the Federal University of Pará by academic support.

Personally, I would like to thank the technician Celso Rafael for their uninterrupted help.

References

- Brotóns, V., R. Tomás, S. Ivorra, and J. C. Alarcón, 2013, Temperature influence on the physical and mechanical properties of a porous rock: San Julian's calcarenite: *Engineering Geology*, **167**, 117–127.
- Figueiredo, D., J. J. S. J. Schleicher, R. R. Stewart, N. Dayur, B. Omoboya, R. Wiley, and A. William, 2013, Shear wave anisotropy from aligned inclusions: ultrasonic frequency dependence of velocity and attenuation: *Geophysical Journal International*, **193**, 475–488.
- Garcia, G. C. R., E. M. B. Santos, and S. Ribeiro, 2011, Effect of the curing time on the stiffness of mortars produced with Portland cement: *Cerâmica*, **57**, 94–99.
- Hudson, J. A., 1981, Wave speeds and attenuation of elastic waves in material containing cracks: *Geophysical Journal of the Royal Astronomical Society*, **64**, 133–150.

- Jansen, D. P., S. R. Carlson, R. P. Young, and D. A. Hutchins, 1993, Ultrasonic imaging and acoustic emission monitoring of thermally induced microcracks in Lac du Bonnet granite: *Journal of Geophysical Research: Solid Earth*, **98**, 22231–22243.
- Kern, H., 1978, The effect of high temperature and high confining pressure on compressional wave velocities in quartz-bearing and quartz-free igneous and metamorphic rocks: *Tectonophysics*, **44**, 185–203.
- Kern, H., and M. Fakhimi, 1975, Effect of fabric anisotropy on compressional-wave propagation in various metamorphic rocks for the range 20–700C at 2 kbars: *Tectonophysics*, **28**, 227–244.
- Martínes, J. M., and D. R. Schmitt, 2011, Investigating anisotropy in rocks by using pulse transmission method.
- Poletto, M., H. L. Junior, and A. J. Zattera, 2014, *Polystyrene : synthesis, characteristics, and applications*: Nova Science Publishers.
- Santos, L. K., J. J. S. de Figueiredo, and C. B. da Silva, 2016, A study of ultrasonic physical modeling of isotropic media based on dynamic similitude: *Ultrasonics*, **70**, 227–237.
- Santos, L. K., J. J. S. de Figueiredo, D. L. Macedo, A. L. de Melo, and C. B. da Silva, 2017, A new way to construct synthetic porous fractured medium: *Journal of Petroleum Science and Engineering*, **156**, 763–768.
- Sobrinho, J., J. de Figueiredo, C. Lima, and L. Santos, 2017, On the temperature dependence of elastic velocities in a synthetic porous vti media: 15th International Congress of the Brazilian Geophysical Society & EXPOGEF, Rio de Janeiro, Brazil, 31 July-3 August 2017, Brazilian Geophysical Society, 249–254.
- Thomsen, L., 1986, Weak elastic anisotropy: *GEOPHYSICS*, **51**, 1954–1966.
- Timur, A., 1977, Temperature dependence of compressional and shear wave velocities in rocks: *GEOPHYSICS*, **42**, 950–956.
- Yan, F., D. Han, Q. Yao, and X. Chen, 2016, Seismic velocities of halite salt: Anisotropy, heterogeneity, dispersion, temperature, and pressure effects: *GEOPHYSICS*, **81**, D293–D301.
- Zhang, L., X. Mao, and A. Lu, 2009, Experimental study on the mechanical properties of rocks at high temperature: *Science in China Series E: Technological Sciences*, **52**, 641–646.